Journal of Molecular Graphics and Modelling 29 (2010) 470–480

Contents lists available at ScienceDirect

Journal of Molecular Graphics and Modelling

journal homepage: www.elsevier.com/locate/JMGM

Structures and spectroscopic properties of nonperipherally and peripherally substituted metal-free phthalocyanines: A substitution effect study based on density functional theory calculations

Aimin Zhong[b], Yuexing Zhang[a,*], Yongzhong Bian[a]

[a] Department of Chemistry, University of Science and Technology Beijing, 30 Xueyuan Road, Beijing 100083, China
[b] Department of Chemistry, Peking University, Beijing 100871, China

ARTICLE INFO

Article history:
Received 26 July 2010
Received in revised form
14 September 2010
Accepted 15 September 2010
Available online 22 September 2010

Keywords:
Metal-free phthalocyanine
Density functional theory
Substitution effect
Electronic structure
Spectroscopic property

ABSTRACT

The molecular structures, molecular orbitals, atomic charges, electronic absorption spectra, and infrared (IR) and Raman spectra of a series of substituted metal-free phthalocyanine compounds with four (**1**, **3**, **5**, **7**) or eight (**2**, **4**, **6**, **8**) methoxyl (**1**, **2**, **5**, **6**) or methylthio groups (**3**, **4**, **7**, **8**) on the nonperipheral (**1**–**4**) or peripheral positions (**5**–**8**) of the phthalocyanine ring are studied by density functional theory (DFT) and time-dependent DFT (TD-DFT) calculations. The calculated structural parameters and simulated electronic absorption and IR spectra are compared with the X-ray crystallography structures and the experimentally observed electronic absorption and IR spectra of the similar molecules, and good agreement between the calculated and experimental results is found. The substitution of the methoxyl or methylthio groups at the nonperipheral positions of the phthalocyanine ring has obvious effects on the molecular structure and spectroscopic properties of the metal-free phthalocyanine. Nonperipheral substitution has a more significant influence than peripheral substitution. The substitution effect increases with an increase in the number of substituents. The methylthio group shows more significant influence than the methoxyl group, despite the stronger electron-donating property of the methoxyl group than the methylthio group. The octa-methylthio-substituted metal-free phthalocyanine compounds have nonplanar structures whose low-lying occupied molecular orbitals and electronic absorption spectra are significantly changed by the substituents. The present systematical study will be helpful for understanding the relationship between structures and properties in phthalocyanine compounds and designing phthalocyanines with typical properties.

1. Introduction

Phthalocyanines have received extensive attention in the past century due to their peculiar and unconventional chemical and physical properties [1]. In addition to their traditional uses as dyes and pigments [1–3] and recently revealed uses as charge carriers in photocopiers and laser printers and materials for optical storage [4–7], many other potential applications are expected for these molecular materials associated with their high thermal and chemical stability, including their use as oxidation catalysts [8], solar cell functional materials [9,10], gas sensors [11,12], nonlinear optical limiting devices [13–15], photodynamic therapy agents [16,17], antimycotic materials [18], and corrosion inhibitors [19].

The structures and properties of the phthalocyanine compounds, including the metal-free phthalocyanine and the phthalocyaninato metal complex, can be tuned by introducing different numbers of substituents with different electronic properties onto the peripheral or nonperipheral positions of the phthalocyanine ring. This property has been well demonstrated by our recent work on 1,8,15,22-tetrakis(alkoxyl)phthalocyanine-containing mono-, bis- and, tris-(phthalocyaninato) metal complexes, namely, $PbPc(\alpha\text{-}OC_5H_{11})_4$, $M(Pc)[Pc(\alpha\text{-}OC_5H_{11})_4]$ (M = Y, Sm–Lu), and $(Pc)M(Pc)M[Pc(\alpha\text{-}OC_5H_{11})_4]$ (M = Sm, Gd, Lu) [20–26]. However, systematic theoretical study describing the complicated effects of the number, properties, and position of the substituents on the structures and properties of the metal-free phthalocyanine at the DFT level is rare. Though one systematic theoretical work on the substitution effect in metal-free phthalocyanine was reported in 2003 [27], the calculations in that work were only based on the MO calculations within the framework of the Pariser–Parr–Pople (PPP) approximation, and the phthalocyanine ring was made perfectly planar with D_{4h} symmetry. Assuming a perfectly planar ring and adopting D_{4h} symmetry omits the effects of the molecular distortion and the central acid hydrogen atoms and, therefore, cannot

* Corresponding author. Tel.: +86 10 6233 4509; fax: +86 10 6233 2462.
E-mail addresses: yxzhang@ustb.edu.cn, zhangyuexing@sdu.edu.cn (Y. Zhang).

1093-3263/$ – see front matter © 2010 Elsevier Inc. All rights reserved.
doi:10.1016/j.jmgm.2010.09.003

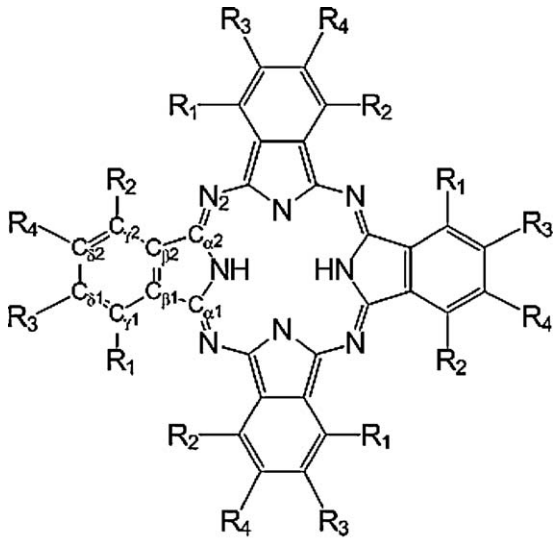

Fig. 1. Molecular structures and atomic labeling of alkoxyl- and sulfoxy-substituted metal-free phthalocyanines **1**–**8**.

correctly reveal the substitution effect in metal-free phthalocyanine. Because there are only two hydrogen atoms bonded to the four isoindole nitrogen atoms and the inner hydrogen atoms in the tetrapyrrole compounds can transfer in the framework of the central hole, the metal-free phthalocyanines are more complicated than the phthalocyaninato metal complexes in their structure and spectroscopic properties, despite the simpler electronic structures of the hydrogen atoms relative to the transition metal atoms. Lee et al. studied the effect of fifteen substituents with different phenyl-ring activating or deactivating properties at one of the eight peripheral positions of the isoindole ring with and without a hydrogen atom and the aza position on the reorganization energy and charge mobility in metal free phthalocyanine at the DFT B3LYP/6-31G(d) level in 2009 [28]. However, the spectroscopic properties of these compounds and the substitution effect of the nonperipheral substitutions were not studied.

In the present paper, we report on the molecular structures, molecular orbitals, atomic charges, electronic absorption spectra, and infrared (IR) and Raman spectra of a series of substituted metal-free phthalocyanine compounds with four or eight methoxyl or methylthio groups on the nonperipheral or peripheral positions of the phthalocyanine ring (**1**–**8**) (Figs. 1 and 2). The influence of the number, property, position, and orientation of the substituents on the structures and properties of the metal-free phthalocyanine compounds has been systematically described. The present work, dealing with the detailed structures, spectroscopic properties, and the substitution effect in the methoxyl- or methylthio-substituted metal-free phthalocyanines with the density functional theory method, will be very useful for understanding the relationship between the structures and the properties of phthalocyanine derivatives with different substituents.

2. Computational details

The hybrid density functional B3LYP (Becke–Lee–Young–Parr composite of exchange-correlation functional) method [29,30] was used for both the geometry optimizations and the property calculations of metal-free phthalocyanine H_2Pc and its substituted derivatives (**1**–**8**). In all cases, the 6-31G* basis set was used. The DFT B3LYP method and the 6-31G* basis set have been widely used in studying the structure and properties of the phthalocyanine compounds, and their efficiency has been proven by numerous previous studies [31–33]. Using the energy-minimized structures generated in the previous step, the normal coordinate analyses were carried out. The charge distribution is calculated using a full natural bond orbital analysis (NBO) population method based on the minimized structure. The primarily calculated vibrational frequencies were not scaled in this work. However, to compare with the experimental results, the available experimental vibrational frequencies were scaled by 1/0.9614 [34]. The electronic absorption spectroscopic calculations were performed by the TDDFT method with 40 excitation states involved. All of the calculations were carried out using the Gaussian03 program [35] in the IBM NAS 300 system in the Shandong Province High-Performance Computing Center.

3. Results and discussion

3.1. Molecular structure

Fig. 1 shows the molecular structures and atomic labeling of the alkoxyl- and sulfoxy-substituted metal-free phthalocyanines **1**–**8**, and Fig. 2 exhibits the optimized structures of these compounds together with their molecular symmetries. Among all of the phthalocyanines, molecules **1**, **3**, **5.1**, **5.2**, **7.1**, and **7.2** have C_{2h} symmetry, whereas molecules **2** and **6** have a higher symmetry of D_{2h} (Fig. 2). In contrast, molecules **4.2** and **8** only have D_2 symmetry, whereas **4.1** has a lower symmetry of C_2. No imaginary vibration is predicted in the IR and Raman vibrational frequency calculations, indicating that the energy-minimized structures for all eleven compounds are true energy minima. The structural parameters of all the substituted compounds **1**–**8** together with those of H_2Pc with D_{2h} symmetry are tabulated in Table S1 (supplementary data).

Table 1 compares the calculated structural parameters of **1** with the X-ray crystallography data of the metal-free 1,8,15,22-tetrakis(2,4-dimethyl-3-pentyloxy)phthalocyanine [36]. Despite the different substituents, the structural parameters of the phthalocyanine macrocycle for **1** correspond well with those of 1,8,15,22-tetrakis(2,4-dimethyl-3-pentyloxy)phthalocyanine. The largest difference in bond length between the calculated and experimental data is only 0.023 Å for the $C_{\gamma1}$–$C_{\delta1}$ bond of isoindole rings with H (isoindole A, Fig. 1) and 0.026 Å for the $C_{\delta1}$–$C_{\delta2}$ bond of isoindole rings without H (isoindole B, Fig. 1). The smallest difference is less than 0.006 and 0.003 Å for isoindole A and isoindole B, respectively. The calculated $C_{\gamma1}$–$O(CH_3)$ bond length for isoindole A and isoindole B is only about 0.005 Å smaller and 0.009 Å larger than the corresponding experimental data, respectively. These results indicate that the results obtained from the DFT calculation at the B3LYP/6-31G(d) level correspond well with the experimentally obtained results. As noted by many other investigators, the bond angle has a much larger error than the bond length in the molecular simulation. This is also true in the present case, as clearly shown in Table 1. The calculated $C_{\alpha1}$–N_1–$C_{\alpha2}$ angle of isoindole rings with H is about 4° larger than the experimental angle, and the $C_{\alpha1}$–N_2–$C_{\alpha2}$ angle is about 5° larger. Similarly to the case of **1**, the calculated molecular structure of **2** also corresponds well with the X-ray crystallography structure of the metal-free 1,4,8,11,15,18,22,25-octakis(2,4-dimethyl-3-pentyloxy)phthalocyanine $H_2Pc(OC_5H_{11})_8$

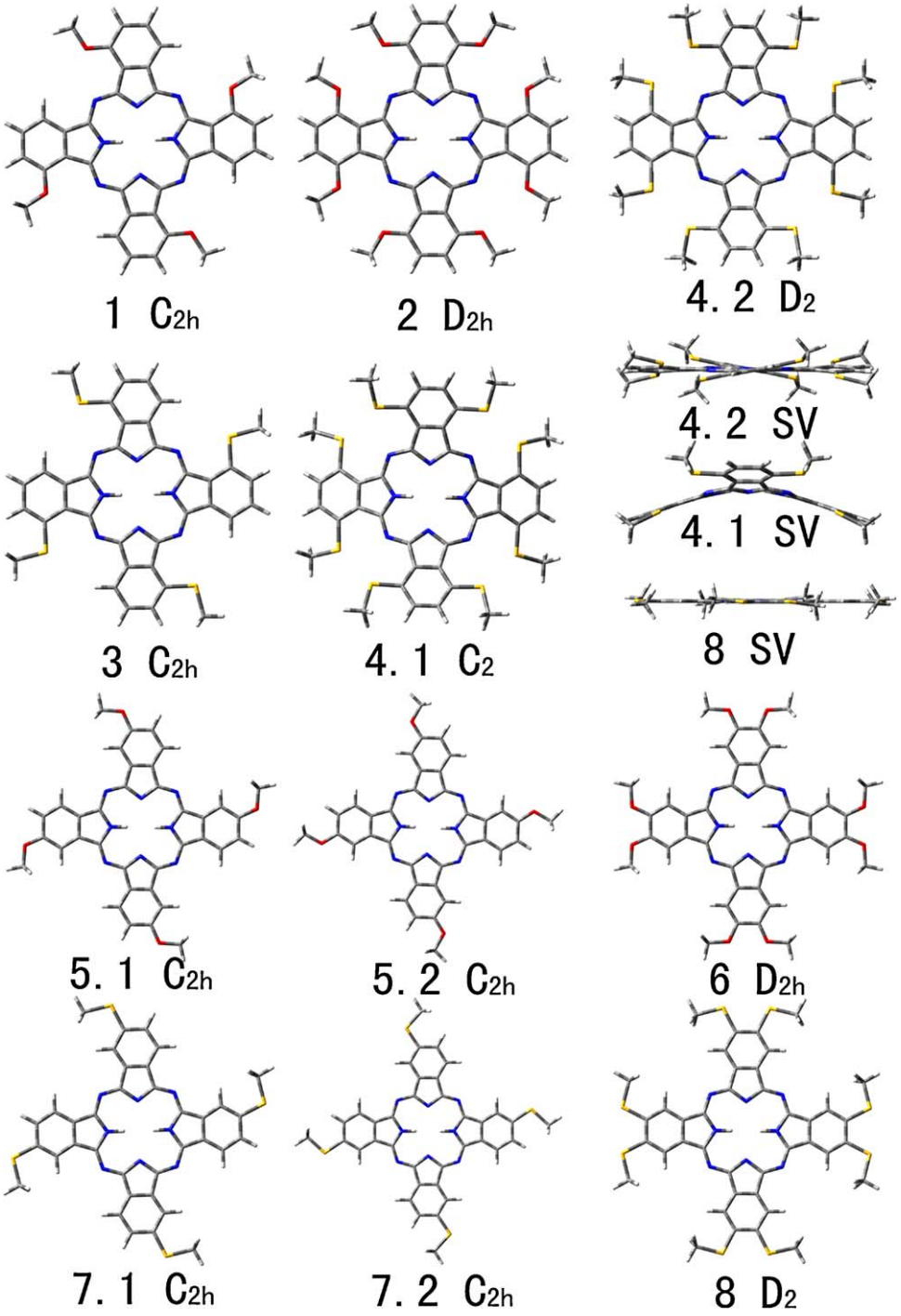

Fig. 2. Optimized molecular structures and symmetries of alkoxyl- and sulfoxy-substituted phthalocyanines **1**–**8** (SV, side view).

(Table 2) [37]. The smallest difference in the bond length between the calculated and experimental data is less than 0.005 Å. Again, the good agreement between the structural data obtained by the DFT method and the experimental results for compound **2** indicates that our calculation method is reliable for simulating the phthalocyanine compounds. A comparison between the calculated molecular structure of H_2Pc and the experimental crystal structure [38] was also performed, and the result is shown in Table S2 (supplementary data). In addition, good consistency between the calculated and experimental data was found.

Similar to the previous results [21], the introduction of four methoxyl groups at the nonperipheral positions of metal-free phthalocyanine, H_2Pc, for compound **1** induces a decrease of molecular symmetry from D_{2h} for H_2Pc to C_{2h}. In the direction of isoindole unit extension, the tetra-substitution with alkoxyl groups at the nonperipheral positions of the phthalocyanine ring also causes isoindole units to twist in **1** due to the steric hindrance of the methoxyl groups. As shown in Tables 1 and S1 (supplementary data), all of the bonds on the same side of the methoxyl group are longer than those on the other side for all isoindole units. For example, the N_1–$C_{\alpha1}$ bond of **1** is about 0.01 Å longer than the N_1–$C_{\alpha2}$ bond in isoindole A. However, the twist of isoindole units is not very large, with the largest difference between the bonds in the same side of the methoxyl group and in the other side being less

Table 1
Comparison of the calculated main structure parameter of **1** with the X-ray crystallography data of metal-free 1,8,15,22-tetrakis(2,4-dimethyl-3-pentyloxy)phthalocyanine.

Parameter[a]	Experimental[b]		Calculated[c]	
	Isoindole with H	Isoindole without H	Isoindole with H	Isoindole without H
N_1–$C_{\alpha1}$	1.375	1.373	1.382	1.368
N_1–$C_{\alpha2}$	1.365	1.364	1.375	1.361
$C_{\alpha1}$–$C_{\beta1}$	1.443	1.456	1.453	1.467
$C_{\alpha2}$–$C_{\beta2}$	1.439	1.447	1.453	1.467
$C_{\beta1}$–$C_{\gamma1}$	1.405	1.412	1.411	1.406
$C_{\beta2}$–$C_{\gamma2}$	1.391	1.388	1.397	1.392
$C_{\beta1}$–$C_{\beta2}$	1.398	1.393	1.413	1.404
$C_{\gamma1}$–$C_{\delta1}$	1.377	1.382	1.400	1.405
$C_{\gamma2}$–$C_{\delta2}$	1.368	1.386	1.389	1.394
$C_{\delta1}$–$C_{\delta2}$	1.389	1.378	1.408	1.404
$C_{\alpha1}$–N_2	1.337	1.329	1.318	1.335
$C_{\alpha2}$–N_2	1.328	1.324	1.317	1.336
$C_{\gamma1}$–O	1.360	1.348	1.355	1.357
$C_{\alpha1}$–N_1–$C_{\alpha2}$	108.7	108.4	112.6	107.0
$C_{\alpha1}$–N_2–$C_{\alpha2}$	123.7	129.5	123.9	124.1

[a] N_1: nitrogen atom joined to the central metal; N_2: nitrogen atom not joined to the central metal; α, β, γ, δ mean carbon atoms in isoindole units beginning from N_1; the subscript 1 on carbon atom refer to carbon atoms at the same side of oxygen atom, the subscript 2 on the carbon atom refers to carbon atoms on the opposite side of oxygen atom, the same side as the hydrogen atoms (see Fig. 1); Å for bond length and degree for bond angle.
[b] Data taken from Ref. [36].
[c] Calculated data using B3LYP/6-31G(d) method (see also Fig. 1 for atomic labeling).

than 0.015 Å. Comparison of the structure parameters of isoindole A with isoindole B indicates that the repulsion between the inner hydrogen atoms makes isoindole A more stout than isoindole B, which can be clearly demonstrated by the larger $C_{\alpha1}$–N_1–$C_{\alpha2}$ angle, longer $C_{\beta1}$–$C_{\beta2}$ and $C_{\delta1}$–$C_{\delta2}$ bonds, whereas the N_1–C_δ distance is shorter for isoindole A than isoindole B.

When eight methoxyl groups are introduced onto the nonperipheral positions of H_2Pc, the D_{2h} symmetry of H_2Pc is retained for **2**. Except for the N_1–C_α bonds and the $C_{\delta1}$–$C_{\delta2}$ bond, all of the bonds in isoindole units of both A and B for **2** are longer than the corresponding bonds for H_2Pc due to the steric hindrance of the methoxyl groups. Due to the increased repulsion associated with the increased number of methoxyl groups, most of the bonds in **2** are longer than the corresponding bonds in **1**. Correspondingly, the distance between isoindole nitrogen atoms of both isoindole A and isoindole B is longer in **1** than in **2**, indicating the enlarged central hole resulting from an increase in the number of substituents.

Due to the impossibility of completely determining the position of the substituents for the peripherally tetrasubstituted phthalocyanine compounds, there are four different isomers without taking into account the inner hydrogen atoms. Because Hanack and co-workers revealed that the C_{4h} (C_{2h} when considering the inner hydrogen atoms) isomer has a very high proportion of 87% [39], only the C_{2h} isomer is considered here. According to the orientation of the methoxyl groups, the C_{2h} isomer of the peripherally tetrasubstituted metal-free phthalocyanine has two configurations named **5.1** and **5.2** (Fig. 2). According to the calculation results, **5.1** is about 0.14 eV more stable than **5.2** due to the weaker repulsion effect between the methoxyl groups and the phthalocyanine ring in the former than in the latter. However, the structure parameters of the phthalocyanine ring of **5.1** and **5.2** are not significantly different. In fact, due to the very small steric hindrance of the methoxyl groups in the peripherally tetrasubstituted phthalocyanine compounds, the methoxyl groups are assumed to be able to rotate along the C_δ–$O(CH_3)$ bond. In contrast to what occurs in **1**, the substituent at the peripheral positions does not induce a twist in isoindole units in the direction of isoindole unit extension. The structural change upon the peripheral tetrasubstitution is also smaller than

Table 2
Comparison of the calculated main structure parameter of **2** with the X-ray crystallography data of metal-free 1,4,8,11,15,18,22,25-octakis(2,4-dimethyl-3-pentyloxy)phthalocyanine.

Parameter[a]	Experimental[b]		Calculated[c]	
	Isoindole with H	Isoindole without H	Isoindole with H	Isoindole without H
N_1–$C_{\alpha1}$	1.440	1.371	1.378	1.364
N_1–$C_{\alpha2}$	1.297	1.423	1.378	1.364
$C_{\alpha1}$–$C_{\beta1}$	1.517	1.436	1.454	1.469
$C_{\alpha2}$–$C_{\beta2}$	1.461	1.417	1.454	1.469
$C_{\beta1}$–$C_{\gamma1}$	1.390	1.391	1.411	1.406
$C_{\beta2}$–$C_{\gamma2}$	1.390	1.389	1.411	1.406
$C_{\beta1}$–$C_{\beta2}$	1.390	1.390	1.415	1.405
$C_{\gamma1}$–$C_{\delta1}$	1.390	1.389	1.395	1.399
$C_{\gamma2}$–$C_{\delta2}$	1.390	1.389	1.395	1.399
$C_{\delta1}$–$C_{\delta2}$	1.390	1.391	1.406	1.402
$C_{\alpha1}$–N_2	1.210	1.336	1.317	1.335
$C_{\alpha2}$–N_2	1.374	1.349	1.317	1.335
$C_{\gamma1}$–O	1.377/1.378	1.378/1.406	1.357	1.360
$C_{\alpha1}$–N_1–$C_{\alpha2}$	118.2	103.1	112.8	107.2
$C_{\alpha1}$–N_2–$C_{\alpha2}$	125.5	120.8‘	124.4	124.4

[a] N_1: nitrogen atom joined to the central metal; N_2: nitrogen atom not joined to the central metal; α, β, γ, δ mean carbon atoms in isoindole units beginning from N_1; the subscript 1 on carbon atom refers to carbon atoms at the same side as the oxygen atom, the subscript 2 on the carbon atom refers to carbon atoms on the opposite side of the oxygen atom, the same side as the hydrogen atoms (see Fig. 1); Å for bond length and degree for bond angle.
[b] Data for $H_2Pc(\alpha\text{-}OC_5H_{11})_8$ taken from Ref. [37].
[c] Calculated data using B3LYP/6-31G(d) method (see also Fig. 1 for atomic labeling).

that upon the nonperipheral tetrasubstitution, indicating the significantly weaker steric hindrance effect of the methoxyl groups at the peripheral positions of the phthalocyanine ring than at the nonperipheral positions.

For the peripherally octasubstituted metal-free phthalocyanine with the methoxyl groups **6**, the primal D_{2h} symmetry of H_2Pc is maintained. Different from the nonperipherally octasubstituted compound **2**, the steric hindrance effect in **6** comes from the two substituents itself of the same isoindole unit instead of from the repulsion between the substituents and the phthalocyanine ring. Due to the small atomic radius of the oxygen atom and the small repulsion between the long-paired electrons of the oxygen atoms, the methoxyl groups (omitting hydrogen) are still in the same plane as the phthalocyanine ring, and compound **6** retains its D_{2h} symmetry. However, the $C_{\delta1}$–$C_{\delta2}$ bonds for both isoindole A and isoindole B of **6** is about 0.028 Å longer than the corresponding bonds of H_2Pc due to the repulsion effect between the methoxyl groups in the same isoindole units. Except for the $C_{\delta1}$–$C_{\delta2}$ bonds, the difference between **6** and H_2Pc is very slight for the other structural parameters, with the largest difference being only 0.008 Å for the $C_{\beta1}$–$C_{\beta2}$ bond, indicating again that the peripheral substituents have a much weaker influence on the structure of phthalocyanine compounds than the substituents at the nonperipheral positions.

Due to the larger atomic radius, the methylthio-substituted metal-free phthalocyanine compounds show different structures in comparison with the methoxyl-group-substituted compounds. Comparison of the structures of **3** and **1** shows that replacing the methoxyl groups with methylthios induces only a very slight change in the structural parameters of the phthalocyanine ring, with the largest difference being less than 0.003 Å. This result indicates that the repulsion between the large methylthio groups and the phthalocyanine ring in the nonperipherally tetrasubstituted phthalocyanines is still relatively small.

When eight methylthio substituents are introduced onto the nonperipheral positions of metal-free phthalocyanine, the methylthio groups cannot be in the same plane of the phthalocyanine ring due to the strong repulsion effect between the neighboring methylthio substituents of the adjacent isoindole units. To reduce the repulsion, the two neighboring substituents between the two adjacent isoindole units will move down and up from the primal phthalocyanine plane, respectively. As can be seen from Fig. 2, there are two possible configurations according to the relative orientation of the two substituents of the same isoindole units: In one configuration, the four methylthio groups of the two opposite isoindole units all move up from the mean phthalocyanine plane while the other four methylthio groups of the other two opposite isoindole units move down, resulting in molecule **4.1** with C_2 symmetry (the saddled configuration), whereas in the other configuration, the two methylthio groups of each isoindole units move up and down, respectively, resulting in molecule **4.2** with D_2 symmetry (the helical configuration). Once the substituents are repulsed up or down from the mean phthalocyanine ring, isoindole units will twist along with the twist of the substituents. The nonperipherally octa-alkoxyl-substituted metal-free phthalocyanines with both the saddled [40–42] and helical [37,43] configuration have been reported experimentally, indicating both the configurations can effectively decrease the repulsion between the neighboring substituents of the two adjacent isoindole units. According to the calculation result, molecule **4.1** is about 0.22 eV more stable than **4.2**, indicating that the saddled configuration is more favorable for decreasing the repulsion effect in the nonperipherally octa-substituted metal-free phthalocyanine compounds than the helical configuration.

The molecular structures of the peripherally tetra-methylthio-substituted metal-free phthalocyanines are very similar to the peripherally tetra-methoxyl-substituted ones. As can be seen from Table S1 (supplementary data), the largest difference for the bond length of **7.1** and **7.2** in comparison with the corresponding bond length of **5.1** and **5.2** is less than 0.002 Å. This result indicates that the size of the substituents on the peripheral position of the tetrasubstituted phthalocyanine compounds have only a minor influence on the structure of the phthalocyanine macrocycle due to the extremely small repulsion between the substituents and the phthalocyanine ring in the peripherally tetrasubstituted phthalocyanines.

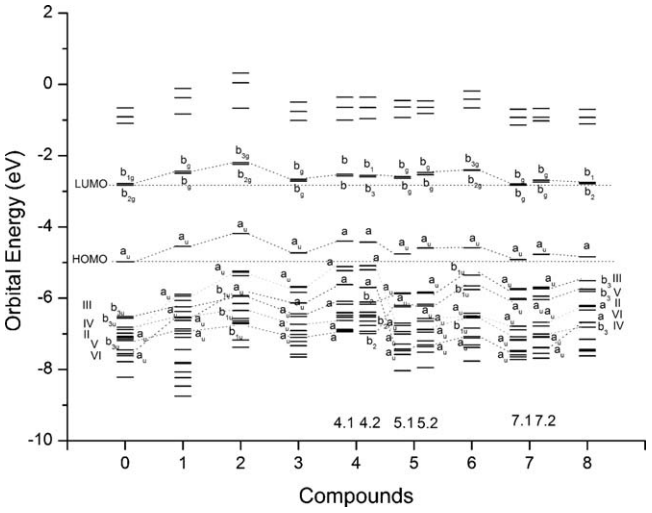

Fig. 3. Energy levels and coincidence relations of the molecular orbitals of **1**–**8** and H_2Pc.

The methylthio groups also cannot be in the plane of the phthalocyanine ring when eight methylthio substituents are introduced onto the peripheral positions of the metal-free phthalocyanine. Unlike the case of **4.1** and **4.2,** in which the repulsion comes from the neighboring methylthio groups of the different isoindole units, the repulsion effect in compound **8** comes from the two methylthio groups of the same isoindole unit. As shown in Table S1 (supplementary data), the $C_{\delta1}$–$C_{\delta2}$ bonds of **8** are lengthened by about 0.027 Å in comparison with those of H_2Pc to reduce the repulsion between the long-pair electrons of the methylthio groups. Even when the $C_{\delta1}$–$C_{\delta2}$ bonds are lengthened to as long as 1.438 Å, there is still significant repulsion between the two methylthio groups of the same isoindole unit for **8**, as revealed by the imaginary frequency of the optimized D_{2h} conformation of compound **8**. To further reduce the repulsion, the two methylthio groups of each isoindole units move up and down toward the mean phthalocyanine plane, forming the helical structure of **8** with D_2 symmetry. In comparison with the D_{2h} structure of the peripherally octa-methoxyl-substituted metal-free phthalocyanine **6**, the D_2 symmetry of the peripherally octa-methylthio-substituted compounds of the metal-free phthalocyanine **8** well represents the effect of the atomic radius of the sulfur family elements in the substituents on the structure of the peripherally octasubstituted phthalocyanines.

3.2. Molecular orbital and atomic charges

Fig. 3 shows the calculated energy levels of the frontier orbitals of compounds **1**–**8** in comparison with H_2Pc. The energy levels of the HOMO and LUMO of the substituted compounds are higher than the corresponding orbitals of the unsubstituted metal-free phthalocyanine H_2Pc, indicating the electron-donating nature of both the methoxyl and methylthio groups. The energy levels of

both the HOMO and LUMO increase with increasing numbers of substituents for both the nonperipherally and peripherally substituted compounds with methoxyl or methylthio substituents. For both the methoxyl- and methylthio-substituted compounds, the HOMO energy level for the nonperipherally substituted compounds is higher than that of the peripherally substituted compounds with the same number of substituents. The HOMO energy level of the peripherally octasubstituted compounds is even lower than that of the nonperipherally tetrasubstituted compounds. These results indicate that the substituents at the nonperipheral positions of the phthalocyanine have a more significant influence on the electronic structure of phthalocyanines than those at the peripheral positions. This finding also corresponds well with the structural change of the phthalocyanine macrocycle upon substitution, as revealed in the molecular structure section. Comparing the methoxyl-substituted metal-free phthalocyanines with the corresponding methylthio-substituted compounds reveals that both the HOMO and LUMO of the methoxyl-substituted metal-free phthalocyanines are higher in energy than of the methylthio-substituted metal-free phthalocyanines, suggesting the stronger electron-donating property of the methoxyl group than the methylthio group. This result corresponds well with not only the Hammett substituent constants of the substituents [44] but also the electrochemical results of the substituted metal-free phthalocyanine compounds [45]. In fact, the difference between the energy of both the HOMO and LUMO of the methylthio-substituted metal-free phthalocyanines and the corresponding energy of H_2Pc is extremely small, in line with the Hammett substituent constant value of the methylthio of almost zero [44]. The energy levels of both the HOMO and LUMO of **5.1** are lower than those of **5.2**, with the HOMO–LUMO energy gap a little larger for the former than for the latter, indicating that **5.1** is more stable than **5.2**. This result corresponds well with the calculated total electronic energy of these two molecules and also holds true for **7.1** and **7.2**. Despite the fact that **4.1** is more stable than **4.2** according to the total electronic energy, **4.1** has a slightly higher orbital energy for the HOMO and LUMO and a smaller HOMO–LUMO energy gap than **4.2**.

Because the LUMO and LUMO+1 orbitals of the metal-free phthalocyanines are not degenerate, unlike the phthalocyaninato metal complexes, and the LUMO+1 and LUMO orbitals distribute on isoindole A and isoindole B, respectively, the energy difference between the LUMO+1 and LUMO orbitals in the metal-free phthalocyanines reflects the difference between isoindole A and isoindole B. As can be seen from Fig. 3, the energy difference between the LUMO and LUMO+1 orbitals for compounds **1**, **3**, **5.2**, and **7.2** is larger than that of the other compounds with the order of **5.2** > **7.2** > **3** > **1**, indicating that the difference between isoindole A and isoindole B for the compounds with only one substituent on each isoindole ring is larger than that of the other compounds. That is, the twist effect on isoindole units caused by the substitution enlarges the difference between isoindole A and isoindole B. The energy difference between the LUMO and LUMO+1 of compound **5.2** is as large as 0.064 eV, indicating the significant difference between isoindole A and isoindole B in **5.2**. In fact, except for compounds **4.2**, **7.1**, **8**, and **6**, the gaps between the LUMO and LUMO+1 (and therefore the difference between isoindole A and isoindole B) of all the other compounds are larger than that of H_2Pc.

Fig. 3 also shows the coincidence relation between the corresponding orbitals of H_2Pc and **1**–**8**, and Fig. S1 (supplementary data) illustrates the maps of these orbitals. As can be seen, in addition to mainly distributing on the carbon atoms, as in H_2Pc, the HOMO orbitals of the substituted metal-free phthalocyanines largely contribute from the p_z orbitals of the oxygen or sulfur atoms of the substituents. In contrast, the contribution from the oxygen or sulfur atoms of the substituents to the LUMO of these compounds is much less than that for the HOMO. This result explains why the HOMO is more significantly influenced by the substituents than the LUMO and the decrease of HOMO–LUMO energy gap upon substitution by the electron-donating groups. However, the HOMO and LUMO of the substituted metal-free compounds **1**-**8** are still dominated by the π orbital of the phthalocyanine ring and do not significantly change in either energy level or orbital shape. In comparison with the HOMO and LUMO (and LUMO+1), the low-lying orbitals of H_2Pc are more significantly influenced by the substituents, and the energy level of some orbitals even reverse. For example, the HOMO−5 orbital of H_2Pc, which mainly distributes on the benzene rings of the phthalocyanine macrocycle with some contribution from the aza nitrogen atoms, significantly increases in energy upon nonperipheral methoxyl- or methylthio-substitution and becomes the HOMO−2 orbital of **1**–**3** and the HOMO−1 orbital of **4.1** and **4.2** due to the very large contribution to this orbital from the oxygen or sulfur atoms of the substituents. In contrast, the HOMO−5 orbital of H_2Pc is still the HOMO−5 or HOMO−6 (for compounds **6** and **8**) orbital in the peripherally substituted compounds. In comparison with the HOMO−5 orbital of H_2Pc, the HOMO−1 orbital of H_2Pc changes to the HOMO−4 or HOMO−5 orbital in the nonperipherally substituted compounds, with the energy and shape changing very little. This orbital, however, becomes the HOMO−1 or HOMO−2 orbital in the peripherally substituted compounds and shows very large contribution from the substituents for orbital distribution.

Table 3 lists the atomic charges (in e), calculated with the NBO population method, of the skeleton atoms for **1**–**8** and H_2Pc. The charge distributed on the central hydrogen atoms for all 11 compounds is very close to that of H_2Pc, with a value of 0.68 e, suggesting a very small influence of the substitution on the charge distribution of the central hydrogen atoms. Except for the N_2 atoms of compounds **1** and **2** and the N_1 atoms of compound **6**, the charges distributed on the N_1, N_2, $C_{\alpha1}$, and $C_{\alpha2}$ atoms of all the substituted compounds are very close to the charge distribution on corresponding atoms in H_2Pc (with charge differences of less than 0.01 e), indicating that the substituents only have a slight influence on the charge distribution of the central 16-atom ring of the phthalocyanine ligand. The change in the charge distribution on the C_β atoms is larger than that on the N_1, N_2, $C_{\alpha1}$, and $C_{\alpha2}$ atoms because of the much smaller distance from the substituents. The oxygen atoms of the methoxyl group all have negative charges around −0.5 e, whereas the sulfur atoms of the methylthio group all show positive charges about 0.3 e, in agreement with the electronic properties of the methoxyl and methylthio groups revealed by the orbital energy level. The methoxyl group has a total negative charge ranging from −0.18 to −0.19 e, whereas the methylthio group shows a total positive charge in the range of 0.23–0.25 e. A comparison between the atomic charges on isoindole A and isoindole B of all the substituted compounds reveals that the N_1 and C_β atoms of isoindole B have more negative charges than isoindole A, whereas the C_α atoms of the former have less positive charges than those of the latter. This trend is identical to that of H_2Pc.

3.3. Electronic absorption spectra

Fig. 4 shows the simulated electronic absorption spectra of compounds **1**–**8** (together with H_2Pc), and Tables S3–S14 (supplementary data) organizes the main peaks, their corresponding oscillator strength, and the nature of electronic transitions. The correlation between the calculated Q bands of **1**–**8** and H_2Pc and the experimental Q bands of the butoxy- or butylthio-substituted metal-free phthalocyanines is shown in Fig. 5. All of the compounds show two split or one combined Q band(s) (I) between 594 and 741 nm, two or three weak bands (II and III) in the range of 377–606 nm, and some coupled Soret bands (IV and V) in the high-energy region. Due to the non-degeneration of the LUMO and LUMO+1 orbitals caused by the inner hydrogen atoms, the

Table 3
NBO atomic charges (in e) for **1**–**8**.

Atom	H	N_1(H)	N_1	$C_{\alpha1}$(H)	$C_{\alpha1}$	$C_{\alpha2}$(H)	$C_{\alpha2}$	$C_{\beta1}$(H)	$C_{\beta1}$	$C_{\beta2}$(H)	$C_{\beta2}$	N_2	X(H)	X	R(H)	R
H_2Pc	0.468	−0.563	−0.610	0.439	0.428	0.439	0.428	−0.080	−0.085	−0.080	−0.085	−0.487	0.253/0.242	0.249/0.239	0.253/0.242	0.249/0.239
1	0.468	−0.565	−0.611	0.440	0.431	0.437	0.424	−0.121	−0.128	−0.065	−0.068	−0.477(9)	−0.497	−0.500	−0.17609	−0.18345
2	0.468	−0.566	−0.611	0.437	0.425	0.437	0.425	−0.104	−0.110	−0.104	−0.110	−0.466	−0.494	−0.496	−0.18281	−0.18912
3	0.469	−0.562	−0.611	0.439	0.431	0.443	0.430	−0.096	−0.102	−0.068	−0.070	−0.488	0.345	0.334	0.24843	0.23468
4.1	0.467	−0.562	−0.610	0.443	0.430	0.443	0.430	−0.084	−0.089	−0.084	−0.089	−0.488	0.358	0.348	0.25617	0.24359
4.2	0.469	−0.563	−0.608	0.442	0.432	0.442	0.432	−0.082	−0.085	−0.082	−0.085	−0.492	0.359	0.346	0.25698	0.24237
5.1	0.468	−0.567	−0.615	0.435	0.425	0.439	0.429	−0.060	−0.063	−0.103	−0.111	−0.490(2)	−0.515	−0.517	−0.19042	−0.19734
5.2	0.468	−0.565	−0.611	0.436	0.425	0.438	0.427	−0.068	−0.071	−0.105	−0.112	−0.490(2)	−0.515	−0.517	−0.19422	−0.19953
6	0.468	−0.571	−0.621	0.435	0.426	0.435	0.426	−0.082	−0.088	−0.082	−0.088	−0.495	−0.505	−0.508	−0.18211	−0.19005
7.1	0.468	−0.565	−0.612	0.438	0.427	0.438	0.428	−0.064	−0.067	−0.093	−0.099	−0.489(90)	0.312	0.305	0.23545	0.22393
7.2	0.468	−0.564	−0.610	0.438	0.427	0.438	0.427	−0.069	−0.072	−0.094	−0.100	−0.489(90)	0.312	0.306	0.2307	0.22177
8	0.468	−0.567	−0.613	0.438	0.427	0.438	0.427	−0.078	−0.083	−0.078	−0.083	−0.493	0.317	0.309	0.24167	0.22974
H_2Pc	0.468	−0.563	−0.610	0.439	0.428	0.439	0.428	−0.080	−0.085	−0.080	−0.085	−0.487	0.253/0.242	0.249/0.239	0.253/0.242	0.249/0.239
1	0.468	−0.565	−0.611	0.440	0.431	0.437	0.424	−0.121	−0.128	−0.065	−0.068	−0.477(9)	−0.497	−0.500	−0.17609	−0.18345
2	0.468	−0.566	−0.611	0.437	0.425	0.437	0.425	−0.104	−0.110	−0.104	−0.110	−0.466	−0.494	−0.496	−0.18281	−0.18912
3	0.469	−0.562	−0.611	0.439	0.431	0.443	0.430	−0.096	−0.102	−0.068	−0.070	−0.488	0.345	0.334	0.24843	0.23468
4.1	0.467	−0.562	−0.610	0.443	0.430	0.443	0.430	−0.084	−0.089	−0.084	−0.089	−0.488	0.358	0.348	0.25617	0.24359
4.2	0.469	−0.563	−0.608	0.442	0.432	0.442	0.432	−0.082	−0.085	−0.082	−0.085	−0.492	0.359	0.346	0.25698	0.24237
5.1	0.468	−0.567	−0.615	0.435	0.425	0.439	0.429	−0.060	−0.063	−0.103	−0.111	−0.490(2)	−0.515	−0.517	−0.19042	−0.19734
5.2	0.468	−0.565	−0.611	0.436	0.425	0.438	0.427	−0.068	−0.071	−0.105	−0.112	−0.490(2)	−0.515	−0.517	−0.19422	−0.19953
6	0.468	−0.571	−0.621	0.435	0.426	0.435	0.426	−0.082	−0.088	−0.082	−0.088	−0.495	−0.505	−0.508	−0.18211	−0.19005
7.1	0.468	−0.565	−0.612	0.438	0.427	0.438	0.428	−0.064	−0.067	−0.093	−0.099	−0.489(90)	0.312	0.305	0.23545	0.22393
7.2	0.468	−0.564	−0.610	0.438	0.427	0.438	0.427	−0.069	−0.072	−0.094	−0.100	−0.489(90)	0.312	0.306	0.2307	0.22177
8	0.468	−0.567	−0.613	0.438	0.427	0.438	0.427	−0.078	−0.083	−0.078	−0.083	−0.493	0.317	0.309	0.24167	0.22974

N_1: nitrogen atom joined to the central metal; N_2: nitrogen atom not joined to the central metal; α, β, γ, δ mean carbon atoms in isoindole units beginning from N_1; H_α: hydrogen atom joined to C_α; H_β: hydrogen atoms joined to C_β; the subscript 1 on the carbon atom refers to carbon atoms at the same side of oxygen atom, and the subscript 2 on the carbon atom refers to carbon atoms on the opposite side of the oxygen atom, the same side as the hydrogen atoms (see Fig. 1).

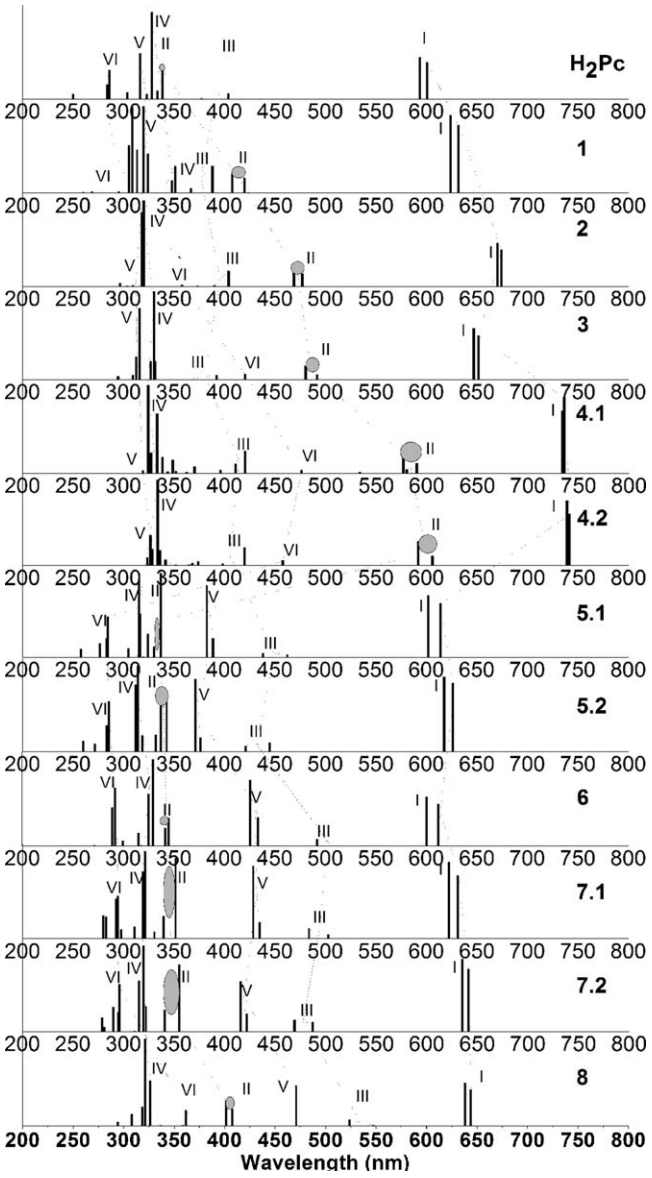

Fig. 4. Simulated electronic absorption spectra of **1**–**8** and H_2Pc.

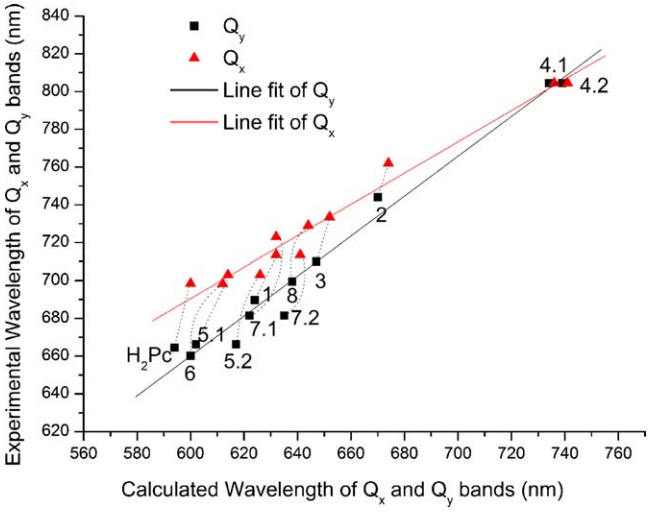

Fig. 5. The correlation between the calculated Q bands of **1**–**8** and H_2Pc and the experimental Q bands of butoxy- or butylthio-substituted metal-free phthalocyanines taken from [27].

Q band splits into two bands attributed mainly to the electronic transition from the HOMO to the LUMO and LUMO+1 orbitals. The two split Q bands of H_2Pc appear at 594 and 600 nm and shift to 624 and 632 nm, 670 and 674 nm, 647 and 652 nm, 734 and 736 nm, 739 and 741 nm, 602 and 614 nm, 617 and 626 nm, 600 and 612 nm, 622 and 632 nm, 635 and 641 nm, and 638 and 644 nm for compounds **1**–**8**, respectively. The substitution redshifts the Q bands due to the decreased HOMO–LUMO (or LUMO+1) energy gap caused by the electron-donating property of the substituents. Similarly (but not identically) to the trend of the HOMO–LUMO energy gap, the average wavelength for the Q bands ($Q_x/2+Q_y/2$) of the substituted compounds decreases in the order of **4.2** > **4.1** > **2** > **3** > **8** > **7.2** > **1** > **7.1** > **5.2** > **5.1** > **6** > H_2Pc, in agreement with the experimentally observed electronic absorption data in THF of the metal-free phthalocyanines substituted with butoxy [27]. It should be mentioned that the calculated energy of the absorption bands in the electronic absorption spectra of these phthalocyanine compounds is not completely coincident with the calculated energy gap of the orbitals included in the electronic transitions because the absorption bands involve many contributions from electronic transitions besides the dominate transition. In addition, as can be seen from Figs. 4 and 5, the splitting of the Q bands increases in the order of **4.2** < **4.1** < **2** < **3** < **8** < **7.2** < H_2Pc < **1** < **5.2** < **7.1** < **5.1** < **6**. This trend generally corresponds with the previous conclusion that the splitting of the Q band of the metal-free phthalocyanines decreases with increasing wavelength of the Q band [27].

According to the calculation results, the weak bands of H_2Pc at 404 and 377 nm (bands III) are mainly due to the electronic transition from the HOMO−1 orbital to the non-degenerate LUMO and LUMO+1 orbitals, respectively. Analysis of the orbital nodes of the HOMO−1 and LUMO (LUMO+1) (Fig. S1, supplementary data) indicates that these bands are due to the $\pi \rightarrow \pi^*$ transition from the benzene rings of the two opposite isoindole units to the other two isoindole units (or π-electron redistribution), the so-called second $\pi \rightarrow \pi^*$ transition band. In detail, the HOMO−1 orbital is mainly distributed on the C_β, C_γ, and N_1 atoms of isoindole B with some contribution from the C_β and C_γ atoms of the other two isoindole rings and the aza N atoms, whereas there is almost no orbital distribution on the N_1(H) atoms and the other carbon atoms. A similar band can also be found in the electronic absorption spectra of ZnPc at 369 nm without splitting [46]. The corresponding bands appear at 388 and 367 nm for **1** due to the electronic transition from the HOMO−4 orbital, at 404 and 358 nm for **2** due to the electronic transition from the HOMO−5 orbital, 392 and 369 nm for **3** due to the electronic transition from the HOMO−5 orbital, 420 and 396 nm for **4.1** due to the electronic transition from the HOMO−5 orbital, and 420 and 398 nm for **4.2** due to the electronic transition from the HOMO−5 orbital. However, probably due to the substituents attached at the peripheral position of the phthalocyanine ring, the distribution of this orbital is significantly disturbed, and the corresponding bands appear at 438 (462), 421 (445), 492 (517), 484 (503), 469 (487), and 524 (547) nm for **5**–**8**, respectively. These bands are mainly due to the electronic transition from the HOMO−2 (for **5.1**, **5.2**, **7.1**, and **7.2**) or HOMO−1 (for **6** and **8**) orbitals to the LUMO and LUMO+1 orbitals.

The two nearly overlapped bands around 338 nm in H_2Pc (bands II) are mainly due to the electronic transition from the HOMO−5 orbital to the nearly degenerate LUMO and LUMO+1 orbitals. The HOMO−5 orbital is mainly distributed on the carbon atoms of the four benzene rings of the phthalocyanine ligand. Although these bands are very strong, they are often covered up by the stronger B bands and are therefore often ignored by researchers. A similar orbital appears as the HOMO−1 or HOMO−2 orbital in the nonperipherally substituted phthalocyanine compounds in combination with the contribution of the p orbital of the O or S atoms. The corresponding bands appear in the range of 408 and 420 nm (for **1**) to 592 and 606 nm (for **4.2**) as weak bands. These bands are assigned as the $n \rightarrow \pi^*$ transition in the alkoxyl- or sulfoxy-substituted phthalocyanines. For example, a $n \rightarrow \pi^*$ transition band is found in the experimental electronic absorption spectra of PbPc(α-OC_5H_{11})$_4$ at 432 nm and is theoretically predicted at 442 nm for both PbPc(α-OC_2H_5)$_4$ and PbPc(α-OC_5H_{11})$_4$ [21]. In comparison with the Q bands, the splitting of these weak bands is more significant, although one of the two bands of some compounds is too weak to be observed. It is worth noting that the weak bands of **4.1** and **4.2** are near or on the long-wavelength side of the Q bands of H_2Pc due to the much higher energy of the HOMO−1 orbital for **4.1** and **4.2** and, thus, the smaller energy gap between the HOMO−1 and LUMO (LUMO+1) orbitals relative to other compounds associated with the saddled and helical structures for **4.1** and **4.2**, respectively, and in particular, the significant contribution from the orbital of the sulfur atoms. Similar bands also exist in the peripherally substituted compounds **5**–**8**, appearing at 337 (330), 343 (337), 345 (342), 351 (340), 355 (341), and 402 (408) nm, respectively, and are due to the electronic transition from the HOMO−5 or HOMO−6 (for **6** and **8**) to the LUMO (LUMO+1) orbitals.

The bands in the Soret region are complex and often include many different $\pi \rightarrow \pi^*$ transitions, rendering the clear assignment of these bands very difficult. As a consequence, only the transitions with the largest contributions are discussed, although in some case the ratio of the largest contribution is no more than 50%. The B band of H_2Pc, appearing at 328 nm (IV), is mainly due to the electronic transition from the HOMO−5 to LUMO+1, and the HOMO−3 to LUMO transition is strongest in the electronic absorption spectrum of H_2Pc. Orbital composition analysis reveals that the HOMO−3 orbital is one of Gouterman's four orbitals with the most distribution over the aza nitrogen atoms, the C_β and C_δ atoms, and a few contributions from isoindole nitrogen atoms. The corresponding band of **1** at 351 nm is mainly due to the electronic transition from the HOMO−6 orbital to LUMO or LUMO+1. It shifts to 320 nm in **2** due to the electronic transition from the HOMO−8 orbital to the LUMO or LUMO+1 orbitals, to 331 nm in **3** due to the electronic transition from the HOMO−7 orbital, to 324 nm in **4.1** due to the electronic transition from the HOMO−11 orbital, and to 334 nm for **4.2** due to the electronic transition from the HOMO−11 orbital. Due to the many-orbital distribution on the C_δ atoms, the HOMO−3 orbital of H_2Pc is more significantly influenced by the substituents at the peripheral positions than the nonperipheral positions, resulting in a more significant increase of the corresponding orbitals in the former than in the latter. As a consequence, the corresponding bands of **5**–**8** shift to 317, 314, 329, 322, 320, and 321 nm due to the electronic transition from the HOMO−7 (for **5**–**7**) or HOMO−9 (for **8**) orbitals to the LUMO or LUMO+1 orbitals, respectively. Due to the significant influence of the substituents at the peripheral positions, this orbital changes into an orbital that is mostly distributed on the eight nitrogen atoms for **6** and **8**.

The other B band of H_2Pc at 317 nm (band V) is mainly due to the electronic transition from the HOMO−9 orbital to the LUMO and/or LUMO+1 orbitals. The HOMO−9 orbital of H_2Pc is mainly distributed on the C_β, C_δ, and the isoindole nitrogen atoms of isoindole A with a few contributions from the aza nitrogen atoms and the isoindole nitrogen atoms of isoindole B. The electronic transitions from similar orbitals induce the electronic absorption bands at 320, 318, 316, 319, and 327 nm for **1**–**4**, respectively. Correspondingly, this B band shifts to 383, 371, 426, 428, 416, and 471 nm for **5**–**8** due to the electronic transition from the HOMO−3 or HOMO−4 orbital to the LUMO or LUMO+1 orbitals.

The N band of H_2Pc appears at 286 nm (band VI), attributed to the electronic transition from the HOMO−11 orbital to the LUMO and/or LUMO+1 orbitals. The HOMO−11 orbital has distribution on all the carbon atoms but almost no contribution from the nitrogen

atoms. However, some orbital nodes on the carbon atoms move to the neighboring nitrogen atoms in some of the substituted phthalocyanine compounds, leading to a change in the orbital energy and a shift of the electronic absorption bands. The HOMO−7 orbital of **1** shows similar features as the HOMO−11 orbital of H_2Pc, from which there is no domain electronic transition. The corresponding bands appearing at 323 nm for **2**, at 420 nm for **3**, 476 nm for **4.1**, and 458 nm for **4.2** are extremely weak. In contrast, the intensity of the corresponding bands in the peripherally substituted phthalocyanines is strong. These bands appear at 284, 285, 292, 293, and 296 nm for **5**–**7**, respectively. This band shifts to 362 nm in compound **8** and is mainly due to the electronic transition from the HOMO−8 orbital.

Our calculated electronic absorption spectra for H_2Pc and **5.1** (or **5.2**), **6**, and **8** correspond well with the available experimental absorption data of H_2Pc and the similar substituted metal-free phthalocyanine compounds, indicating that the TD-DFT method can reasonably reproduce the electronic absorption spectra of phthalocyanine compounds. Corresponding to the two sharp peaks experimentally predicted in the visible region at 686 nm (Q_x) and 622 nm (Q_y), the less intense broad band centered at 340 nm (named the Soret or B band), and the other bands (N, L, and C) below 280 nm [47], the calculated electronic transitions appear at 600, 594, 328, and 286 nm for the Q_x, Q_y, B, and N bands, respectively. The calculated bands appearing at 602 and 614 nm (Q bands), 383 and 389 nm (IV), 316 and 317 nm (V), and 283 and 284 nm (VI) for **5.1** also correspond well with the observed experimental peaks at 659 and 693 nm (Q bands), 392 nm (IV), 339 nm (V), and 290 nm (VI) for metal-free 2(3),9(10),16(17),23(24)-tetrakis(2-isopropyl-5-methylcyclohexoxyl)phthalocyanine [48]. This finding is also true for compound **5.2**. The calculated absorption bands of **5.1** and **5.2** can also find analogs in the electronic absorption spectra of some other peripherally tetrasubstituted metal-free phthalocyanines with the alkoxyl-containing groups [49–53]. Novel metal-free phthalocyanines containing four 19-membered dithiadiazadioxa macrocycles show split Q bands at 707 and 689 nm and B bands at 334 and 281 nm [54], which correspond to the calculated electronic absorption bands of **6** at 612 and 600 nm and 329 and 292 nm, respectively. The calculated electronic absorption spectra of **6** can also find analogs in the recorded electronic absorption spectra of the symmetrically tetrasubstituted metal-free phthalocyanine with four 14-membered dioxadithia macrocycles, each of which is attached to a 15-membered crown ether, at 708 and 641 and 292 nm [55]. The calculated electronic absorption bands at 321, 362, 402, 471, 638, and 644 nm in the electronic absorption spectrum of **8** are similar to the observed bands at 296, 326, 368, 449, 656, and 707 nm for the metal-free phthalocyanine containing four 27-membered diazaheptathia macrocyclic moieties on the peripheral positions [56], respectively, and can also correspond with the absorption bands of the metal-free phthalocyanine containing four 18-membered tetrathiadiaza macrocycles moieties on the peripheral positions [57] and the metal-free phthalocyanine bearing eight 16-membered tetrathiamonoaza macrocycles in the peripheral positions [58].

3.4. IR spectra

The calculated IR spectra of **1**–**4** are shown in Fig. S4 (supplementary data), and those of **5**–**8** are shown in Fig. S5 (supplementary data). The calculated data are fit to Lorentzian lineshapes. As shown in the figures, the vibrational modes in the spectra of **1**–**8** are more complicated than the spectrum of H_2Pc due to the introduction of the methoxyl and methylthio groups. The N–H stretching vibration in H_2Pc at 3559 cm^{-1} shows a very slight change in the substituted metal-free phthalocyanines, shifting to 3560 cm^{-1} in **1**, 3561 cm^{-1} in **2**, 3562 cm^{-1} in **3**, 3561 cm^{-1} in **4.2**, 3563 cm^{-1} in **5.1**, 3561 cm^{-1} in **5.2**, 3566 cm^{-1} in **6**, 3562 cm^{-1} in **7.1**, 3561 cm^{-1} in **7.2**, and 3563 cm^{-1} in **8**. This result is in agreement with the very small structural differences for N–H bonds between H_2Pc and the substituted compounds. Most likely due to the saddle configuration with lower C_2 symmetry, a very weak N–H symmetric stretching vibration is found in the IR spectrum of **4.1** at 3630 cm^{-1}, and the N–H unsymmetric stretching peak in **4.1** shifts significantly to 3577 cm^{-1}. In addition to the peaks due to the C–H stretching of the benzene ring in the range of 3180–3250 cm^{-1}, several new peaks appear on the lower energy side of these peaks in the spectra of **1**–**8** and are clearly due to the symmetrical and asymmetrical C–H stretching modes of the methoxyl and methylthio groups. The calculated N–H stretching vibration in H_2Pc at 3559 cm^{-1} in this work corresponds well with both the previous calculation results at 3561 cm^{-1} [59] and the experimental data at 3404 (3273/0.9614) cm^{-1} [60]. The calculated N–H stretching vibration in **5.1** at 3563 cm^{-1} in this work also agrees well with the corresponding N–H vibration in other peripherally tetrasubstituted metal-free phthalocyanines, with the alkoxyl-containing groups in the range of 3375–3428 cm^{-1} [49–53]. This agreement also holds for compound **6** [54,55]. These results indicate that the calculated IR spectra using the B3LYP/6-31G* method show good consistency with the experimental data.

The vibration peaks below 1800 cm^{-1} for these complexes are quite complicated and are actually the mixture of many interrelated vibrational modes. The spectra of **1**–**8** also show significant differences from the H_2Pc spectrum in this region, and the spectra of **1**–**8** have different characteristics. The strongest peak for H_2Pc at 1092 cm^{-1} due to isoindole stretching shifts to 1072, 1078, 1092, 1115, 1096, 1074, 1095, 1079, 1080, 1078, and 1078 cm^{-1} for **1**–**8**, respectively. Corresponding to the weak peaks around 1300 cm^{-1} due to the C–H in plane bending vibrations in the spectrum of H_2Pc, several strong peaks due to C(Ph)–O–C(CH_3) stretching coupled with benzene deformation and C(Ph)–H in-plane bending vibrations appear in the IR spectra of the methoxyl-substituted metal-free phthalocyanines. The peak at 1321 cm^{-1} in the spectrum of **1** shifts to 1327 cm^{-1} in **2** and becomes the strongest peak. The corresponding peaks appear at 1315, 1314, and 1318 cm^{-1} for **5.1**, **5.2**, and **6**, respectively. In comparison with the methoxyl-substituted compounds, the C(Ph)–S–C(CH_3) stretching vibration peaks are much weaker and shift to lower energy. The intensity of the benzene stretching vibrational peaks around 1650 cm^{-1} in the spectra of the substituted compounds is much stronger than that of H_2Pc due to the involvement of the vibrational modes of the methoxyl and methylthio groups. Despite the complexity in the IR vibrational spectra of the substituted phthalocyanines, most of the vibrational modes can be identified and assigned by comparison with those of the unsubstituted analog according to the calculation results.

3.5. Raman spectra

The simulated Raman spectra of **1**–**4** and **5**–**8** are shown in Figs. S6 and S7 (supplementary data), respectively. Similar to the IR spectra, the calculated Raman data are fit to Lorentzian lineshapes. The strongest peaks of all the substituted compounds are the C–N_2 asymmetric stretching mixed with the C–C and C–N_1 stretching, appearing at 1612, 1607, 1610, 1582, 1583, 1609, 1611, 1607, 1608, 1610, and 1607 cm^{-1} for **1**–**8**, respectively, which contain no contribution from the vibrations of the substituents and shift to lower energy with an increase in the substitution number and with a decrease in the substituent's electron-donating property. With the assistance of the animated pictures produced from the normal coordinates, the other Raman peaks can also be easily assigned. As in the IR spectra, there are more peaks in the Raman spectra of **1**–**8**

than in H_2Pc due to the introduction of the substituents and the diminished molecular symmetry. It is worth noting that the calculated Raman spectrum of H_2Pc at the same B3LYP/6-31G* level as used in this work has been compared to the experimental spectrum emitting at a wavelength of 632.8 nm in a previous work [61], indicating the less-than-good but acceptable correlation between the calculated Raman wavenumbers and the experimentally observed wavenumbers.

4. Conclusion

An accurate description of the molecular structures, molecular orbital, atomic charges, electronic absorption spectra, and IR and Raman spectra of a series of substituted metal-free phthalocyanine compounds has been provided by DFT and TDDFT calculations. Introducing four methoxyl or methylthio groups at the nonperipheral positions of metal-free phthalocyanine H_2Pc induces a decrease of the molecular symmetry from D_{2h} for H_2Pc to C_{2h} for **1** and **3** and the twist of isoindole units in the direction of isoindole unit extension. Although the nonperipherally octa-methoxyl-substituted derivative of H_2Pc (**2**) maintains a planar molecular structure with D_{2h} symmetry, the nonperipherally octa-methylthio-substituted derivative **4** takes the C_2-symmetry saddled configuration or D_2-symmetry helical configuration due to the strong repulsion effect between the neighboring methylthio substituents of the different isoindole units. Except for the peripherally octa-methylthio-substituted compound **8**, which takes a helical structure with D_2 symmetry due to the strong repulsion between the neighboring methylthio groups of the same isoindole ring, the other peripherally substituted compounds of metal-free phthalocyanine retain a planar structure and are less influenced by the substituents than the nonperipherally substituted phthalocyanine derivatives. The electron-donating methoxyl or methylthio groups raise the energy level of the HOMO and LUMO of H_2Pc in all of the substituted compounds **1**–**8**, with the former increasing more significantly than the latter and both increasing with the increase of the number of substituents. The substitution also induces a change in the energy level of some low-lying orbitals and even reverses the ordering of some orbitals, inducing significantly different electronic absorption spectra between H_2Pc and the substituted derivatives and between the nonperipherally and peripherally substituted compounds. The IR and Raman spectra of H_2Pc and **1**–**8** are compared with the calculation results.

Acknowledgements

Financial support from the Natural Science Foundation of China, Beijing Municipal Commission of Education, China Postdoctoral Science Foundation (20090460210), and University of Science and Technology Beijing is gratefully acknowledged. We are also grateful to the Shandong Province High Performance Computing Center for a grant of computer time.

Appendix A. Supplementary data

Calculated molecular structural parameters of **1**–**8**, orbital maps of orbitals included in the excitation transitions of **1**–**8**, simulated electronic absorption spectra of **1**–**8** and H_2Pc, simulated IR and Raman spectra of **1**–**8**, and all of the excitations and the corresponding oscillator strengths and major transition orbital contributions of **1**–**8** and H_2Pc.

Supplementary data associated with this article can be found, in the online version, at doi:10.1016/j.jmgm.2010.09.003.

References

[1] N.B. Mckeown, Phthalocyanine Materials: Synthesis, Structure and Function, Cambridge University Press, Cambridge, England, 1998.
[2] A.B.P. Lever, C.C. Leznoff, Phthalocyanine: Properties and Applications, vols. 1–4, VCH Publishers, New York, 1989–1996.
[3] K.M. Kadish, K.M. Smith, R. Guilard, The Porphyrin Handbook, vols. 1–20, Academic Press, San Diego, CA, 2000–2003.
[4] P. Gregory, High-technology Applications of Organic Colorants, Plenum Press, New York, 1991.
[5] P. Gregory, Industrial applications of phthalocyanines, J. Porphyrins Phthalocyanines 4 (2000) 432–437.
[6] R. Ao, L. Kilmmert, D. Haarer, Present limits of data storage using dye molecules in solid matrices, Adv. Mater. 7 (1995) 495–499.
[7] D. Birkett, Creating an information revolution, Chem. Ind. (2000) 178–181.
[8] F.H. Moser, A.L. Thomas, The Phthalocyanines: Manufacture and Applications, vols. 1–2, CRC Press, Boca Raton, FL, 1983.
[9] D. Wöhrle, D. Meissner, Organic solar cells, Adv. Mater. 3 (1991) 129–138.
[10] H. Eichhorn, Mesomorphic phthalocyanines, tetraazaporphyrins, porphyrins and triphenylenes as charge-transporting materials, J. Porphyrins Phthalocyanines 4 (2000) 88–102.
[11] J.D. Wright, Gas adsorption on phthalocyanines and its effects on electrical properties, Prog. Surf. Sci. 31 (1989) 1–60.
[12] A.W. Snow, W.R. Barger, in: C.C. Leznoff, A.B.P. Lever (Eds.), Phthalocyanines: Properties and Applications, VCH Publishers, New York, 1989, pp. 341–392.
[13] H.S. Nalwa, J.S. Shirk, in: C.C. Leznoff, A.B.P. Lever (Eds.), Phthalocyanines: Properties and Applications, VCH Publishers, New York, 1996, pp. 79–182.
[14] J.S. Shirk, R.G.S. Pong, S.R. Flom, H. Heckmann, M. Hanack, Effect of axial substitution on the optical limiting properties of indium phthalocyanines, J. Phys. Chem. A 104 (2000) 1438–1449.
[15] G. de la Torre, P. Vázquez, F. AgullóPez, T. Torres, Phthalocyanines and related compounds: organic targets for nonlinear optical applications, J. Mater. Chem. 8 (1998) 1671–1683.
[16] E.A. Lukyanets, Phthalocyanines as photosensitizers in the photodynamic therapy of cancer, J. Porphyrins Phthalocyanines 3 (1999) 424–432.
[17] H. Ali, J.E. van Lier, Metal complexes as photo- and radiosensitizers, Chem. Rev. 99 (1999) 2379–2450.
[18] B. Cosomelli, G. Roncuccin, D. Dei, L. Fantetti, F. Ferroin, M. Ricci, D. Spinelli, Synthesis and antimycotic activity of new unsymmetrical substituted zinc phthalocyanines, Tetrahedron 59 (2003) 10025–10030.
[19] H.I. Beltrán, R. Esquive, A. Sosa-Sánchez, J.L. Sosa-Sánchez, H. Höpfl, V. Barba, N. Farfan, M.G. Garcia, O. Olivares-Xometl, L.S. Zamudio-Rivera, Microwave assisted stereoselective synthesis of cis-substituted tin^{IV} phthalocyanine dicarboxylates. Application as corrosion inhibitors, Inorg. Chem. 43 (2004) 3555–3557.
[20] Y. Bian, L. Li, J. Dou, D.Y.Y. Cheng, R. Li, C. Ma, D.K.P. Ng, J. Jiang, Synthesis, structure, spectroscopic properties, and electrochemistry of (1,8,15,22-tetrasubstituted phthalocyaninato)lead complexes, Inorg. Chem. 43 (2004) 7539–7544.
[21] Y. Zhang, X. Zhang, Z. Liu, Y. Bian, J. Jiang, Structures and properties of 1,8,15,22-tetrasubstituted phthalocyaninato-lead complexes: the substitution effect study based on density functional theory calculations, J. Phys. Chem. A 109 (2005) 6363–6370.
[22] A. Zhong, Y. Bian, Y. Zhang, Semiconductor performance of phthalocyaninato lead complex and its nonperipherally substituted derivatives for organic field effect transistors: density functional theory calculations, J. Phys. Chem. C 114 (2010) 3248–3255.
[23] X. Cai, Y. Zhang, X. Zhang, J. Jiang, Structures and properties of 2,3,9,10,16,17,23,24-octasubstituted phthalocyaninato-lead complexes: the substitution effect study on the basis of density functional theory calculations, J. Mol. Struct. (Theochem) 801 (2006) 71–80.
[24] Y. Bian, R. Wang, J. Jiang, C.H. Lee, J. Wang, D.K.P. Ng, Synthesis, spectroscopic characterisation and structure of the first chiral heteroleptic bis(phthalocyaninato) rare earth complexes, Chem. Commun. (2003) 1194–1195.
[25] Y. Bian, R. Wang, D. Wang, P. Zhu, R. Li, J. Dou, W. Liu, C.F. Choi, H.S. Chan, C. Ma, D.K.P. Ng, J. Jiang, Synthesis, structure, and spectroscopic and electrochemical properties of heteroleptic bis(phthalocyaninato) rare earth complexes with a C_4 symmetry, Helv. Chim. Acta 87 (2004) 2581–2596.
[26] Y. Bian, L. Li, D. Wang, C.F. Choi, D.F.F. Cheng, P. Zhu, R. Li, J. Dou, R. Wang, N. Pan, C. Ma, D.K.P. Ng, N. Kobayashi, J. Jiang, Synthetic, structural, spectroscopic, and electrochemical studies of heteroleptic tris(phthalocyaninato) rare earth complexes, Eur. J. Inorg. Chem. (2005) 2612–2618.
[27] N. Kobayashi, H. Ogata, N. Nonaka, E.A. Luk'yanets, Effect of peripheral substitution on the electronic absorption and fluorescence spectra of metal-free and zinc phthalocyanines, Chem. Eur. J. 9 (2003) 5123–5134.
[28] C. Lee, K. Sohlberg, The effect of substitution on reorganization energy and charge mobility in metal free phthalocyanine, Chem. Phys. 367 (2010) 7–19.
[29] C. Lee, W. Yang, R.G. Parr, Development of the Colle–Salvetti correlation-energy formula into a functional of the electron density, Phys. Rev. B 37 (1988) 785–789.
[30] A.D. Becke, Density-functional thermochemistry. III. The role of exact exchange, J. Chem. Phys. 98 (1993) 5648.
[31] D. Qi, Y. Zhang, X. Cai, J. Jiang, M. Bai, Inner hydrogen atom transfer in benzo-fused low symmetrical metal-free tetraazaporphyrin and phthalocyanine analogues: density functional theory studies, J. Mol. Graph. Model. 27 (2009) 693–700.

[32] Y. Zhang, P. Yao, X. Cai, H. Xu, X. Zhang, J. Jiang, Density functional theory study of the inner hydrogen atom transfer in metal-free porphyrins: meso-substitution effects, J. Mol. Graph. Model. 26 (2007) 319–326.
[33] J. Andzelm, A.M. Rawlett, J.A. Orlicki, J.F. Snyder, K.K. Baldridge, Optical properties of phthalocyanine and naphthalocyanine compounds, J. Chem. Theory Comput. 3 (2007) 870–877.
[34] R.D. Johnson III (Ed.), NIST Computational Chemistry Comparison and Benchmark Database, NIST Standard Reference Database, Number 101, Release 10, May 2004 http://srdata.nist.gov/cccbdb.c.
[35] M.J. Frisch, et al., Gaussian 03, Revision B.05, Gaussian, Inc., Pittsburgh, PA, 2003.
[36] W. Liu, C.-H. Lee, H.-W. Li, C.K. Lam, J. Wang, T.C.W. Mak, D.K.P. Ng, Formation and crystal structure of an unexpected inclusion complex of a metal-free phthalocyanine and oxalic acid, Chem. Commun. (2002) 628–629.
[37] M.P. Donzello, C. Ercolani, A.A. Gaberkorn, E.V. Kudrik, M. Meneghetti, G. Marcolongo, C. Rizzoli, P.A. Stuzhin, Synthesis, X-ray crystal structure, uv/visible linear and nonlinear (optical limiting) spectral properties of symmetrical and unsymmetrical porphyrazines with annulated 1,2,5-thiadiazole and 1,4-diamyloxybenzene moieties, Chem. Eur. J. 9 (2003) 4009–4024.
[38] R.B. Hammond, K.J. Roberts, R. Docherty, M. Edmondson, R. Cairns, X-form metal-free phthalocyanine: crystal structure determination using a combination of high-resolution X-ray powder diffraction and molecular modelling techniques, J. Chem. Soc. Perkin Trans. 2 (1996) 1527–1528.
[39] C. Rager, G. Schmid, M. Hanack, Influence of substituents reaction conditions and central metals on the isomer distributions of 1(4)-tetrasubstituted phthalocyanines, Chem. Eur. J. 5 (1999) 280–288.
[40] Y. Gao, Y. Chen, R. Li, Y. Bian, X. Li, J. Jiang, Nonperipherally octa(butyloxy)-substituted phthalocyanine derivatives with good crystallinity: effects of metal–ligand coordination on the molecular structure, internal structure, and dimensions of self-assembled nanostructures, Chem. Eur. J. 15 (2009) 13241–13252.
[41] N.B. McKeown, H. Li, M. Helliwell, A non-planar, hexadeca-substituted, metal-free phthalocyanine, J. Porphyrins phthalocyanines 9 (2005) 841–845.
[42] S.M. Gorun, J.W. Rathke, M.J. Chen, Long-range solid-state ordering and high geometric distortions induced in phthalocyanines by small fluoroalkyl groups, Dalton Trans (2009) 1095–1097.
[43] M.J. Cook, J. McMurdo, A.K. Powell, X-Ray crystal structure of 1,4,8,11,15,18,22,25-octa-iso-pentyloxyphthalocyanine, J. Chem. Soc. Chem. Commun. (1993) 903–904.
[44] C. Hansch, A. Leo, R.W. Taft, A survey of Hammett substituent constants and resonance and field parameters, Chem. Rev. 91 (1991) 165–195.
[45] R. Li, X. Zhang, P. Zhu, D.K.P. Ng, N. Kobayashi, J. Jiang, Electron-donating or -withdrawing nature of substituents revealed by the electrochemistry of metal-free phthalocyanines, Inorg. Chem. 45 (2006) 2327–2334.
[46] L. Wan, Y. Zhang, D. Qi, J. Jiang, Structures and properties of 1,8,15,22-tetrasubstituted phthalocyaninato zinc and nickel complexes: Substitution and axially coordination effects study based on density functional theory calculations, J. Mol. Graph. Modell. 28 (2010) 842–851.
[47] E. Orti, J.L. Brédas, C. Clarisse, Electronic structure of phthalocyanines: theoretical investigation of the optical properties of phthalocyanine monomers, dimers, and crystals, J. Chem. Phys. 92 (1990) 1228.
[48] W. Lv, X. Wu, Y. Bian, J. Jiang, X. Zhang, Helical fibrous nanostructures self-assembled from metal-free phthalocyanine with peripheral chiral menthol units, ChemPhysChem 10 (2009) 2725–2732.
[49] Z. Bıyıklıoğlu, H. Kantekin, İ. Acar, The synthesis and characterization of new organosoluble long chain-substituted metal-free and metallophthalocyanines by microwave irradiation, Inorg. Chem. Commun. 11 (2008) 1448–1451.
[50] Z. Bıyıklıoğlu, H. Kantekin, The synthesis, using microwave irradiation and characterization of novel, organosoluble metal-free and metallophthalocyanines substituted with flexible crown ether moieties, Dyes Pigments 80 (2009) 17–21.
[51] Z Bıyıklıoğlu, E.T. Güner, S. Topçu, H. Kantekin, Synthesis, characterization and electrochemistry of a new organosoluble metal-free and metallophthalocyanines, Polyhedron 27 (2008) 1707–1713.
[52] Z. Bıyıklıoğlu, H. Kantekin, Microwave assisted synthesis and characterization of novel metal-free and metallophthalocyanines containing four pyridyl groups, Transit. Met. Chem. 32 (2007) 851–856.
[53] A. Bilgin, Ç. Yağcı, A. Mendi, U. Yıldız, Synthesis and characterization of new metal-free and metallophthalocyanines fused α-methylferrocenylmethoxyl units, J. Incl. Phenom. Macrocycl. Chem. 67 (2010) 377–383.
[54] Z. Bıyıklıoğlu, H. Kantekin, A novel metal-free and metallophthalocyanines containing four 19-membered dithiadiazadioxa macrocycles by microwave irradiation: Synthesis and characterization, J. Organomet. Chem. 693 (2008) 505–509.
[55] A. Bilgin, B. Ertem, Y. Gök, The synthesis and characterization of a new metal-free phthalocyanine substituted with four diloop macrocyclic moieties, Tetrahedron Lett. 44 (2003) 3829–3833.
[56] H.Z. Gök, H. Kantekin, Y. Gök, G. Herman, The synthesis and characterization of new metal-free and metallophthalocyanines containing four 27-membered diazaheptathia macrocycles, Dyes Pigments 75 (2007) 606–611.
[57] H. Kantekin, G. Dilber, A. Nas, Microwave-assisted synthesis and characterization of a new soluble metal-free and metallophthalocyanines peripherally fused to four 18-membered tetrathiadiaza macrocycles, J. Organomet. Chem. 695 (2010) 1210–1214.
[58] B. Ertem, B. Bilgin, Y. Gök, H. Kantekin, The synthesis and characterization of novel metal-free and metallophthalocyanines bearing eight 16-membered macrocycles, Dyes Pigments 77 (2008) 537–544.
[59] X. Zhang, Y. Zhang, J. Jiang, Isotope effect in the infrared spectra of free-base phthalocyanine and its N,N-dideuterio-derivative: density functional calculations, Vib. Spectrosc. 33 (2003) 153–161.
[60] M.P. Sammes, The infrared spectrum of phthalocyanine: assignment of N–H modes, J. Chem. Soc. Perkin Trans. 2 (1972) 160–162.
[61] X. Zhang, M. Bao, N. Pan, Y. Zhang, J. Jiang, IR and Raman vibrational assignments for metal-free phthalocyanine from density functional B3LYP/6-31G(d) method, Chin. J. Chem. 22 (2004) 325–332.